Available online at www.sciencedirect.com
ScienceDirect
Antiviral Research 75 (2007) 210–218
Antiviral Research
www.elsevier.com/locate/antiviral

# Molecular basis of antagonism between K70E and K65R tenofovir-associated mutations in HIV-1 reverse transcriptase

R.M. Kagan [a,*], T.-S. Lee [b], L. Ross [c], R.M. Lloyd Jr. [d], M.A. Lewinski [a], S.J. Potts [a]

[a] *Quest Diagnostics Nichols Institute, San Juan Capistrano, CA 92675, United States*
[b] *Consortium for Bioinformatics and Computational Biology, and Department of Chemistry, University of Minnesota, P.O. Box 14800, Minneapolis, MN 55414, United States*
[c] *Glaxo SmithKline, Research Triangle Park, NC 27709, United States*
[d] *Research Think Tank Inc., Alpharetta, GA 30004, United States*

Received 24 November 2006; accepted 13 March 2007

**Abstract**

The K70E mutation in HIV-1 reverse transcriptase was observed in 10% of virologic non-responders of the abacavir/lamivudine/tenofovir arm of ESS30009, alone, or in mixtures with K65R by population sequencing. Clonal analysis of six ESS30009 K70E isolates failed to identify double mutants carrying K65R + K70E. Site-directed K70E mutants had a replication capacity of 97 ± 29%, but only 2.4 ± 0.9% for K65R + K70E and 0.01% for K65R + K70E + M184V mutants. K65R + K70E phenotypic fold changes for abacavir, lamivudine and tenofovir were comparable to reported values for K65R alone. In molecular dynamic simulations, the ε-amino group of K65 was positioned 2.7 ± 0.1 Å from the γ-phosphate of the dTTP ligand and stabilized the triphosphate. In the R65 mutant, this distance increased to 4.2 ± 0.4 Å and the interaction energy with the ligand was less favorable, but the K70 ε-amino group was repositioned closer to the γ-phosphate and had a more favorable interaction energy. In the double mutant, E70 could not stabilize the γ-phosphate, resulting in a more severe defect. The net effect of the atomic-level changes in the double mutant may be to destabilize the pyrophosphate leaving group of the ligand, more severely affecting the catalytic rate of the polymerization reaction than the R65 single mutation.


*Keywords:* HIV-1; Reverse transcriptase; Tenofovir; K65R; K70E; Molecular dynamics

## 1. Introduction

The HIV-1 reverse transcriptase (RT) mutation K65R is associated with reduced susceptibility to the nucleotide RT inhibitor (NtRTI) tenofovir disoproxil fumarate (Sarafianos et al., 1999; Wainberg et al., 1999) and other non-azido-containing nucleoside RT inhibitors (NRTI) (Parikh et al., 2005, 2006). Since the approval of tenofovir for clinical use in October 2001, an increasing prevalence of K65R in clinical HIV-1 genotypic testing databases has been reported (Faruki et al., 2004; Kagan et al., 2004; Camacho et al., 2006). K65R has also been observed at a high frequency in studies of patients experiencing virologic failure on triple-NRTI regimens of tenofovir and lamivudine combined with abacavir (Gallant et al., 2005; Khanlou et al., 2005; Landman et al., 2005) and with tenofovir combined with didanosine-containing regimens (Leon et al., 2005; Maitland et al., 2005; Torti et al., 2005). We previously reported that the rare K70E mutation, which is associated with reduced susceptibility to the nucleoside analog adefovir (Cherrington et al., 1996; Miller et al., 2001), has also increased in prevalence since the introduction of tenofovir: from 0.18% of antiretroviral (ARV)-resistant samples in 1999–2001 to 0.43% in 2002–2004 (Kagan et al., 2005). K70E has also been reported in a small number of patients failing on antiretroviral regimens containing tenofovir (Delaugerre et al., 2005; Rouse et al., 2005; Lloyd et al., 2005).

In the Virco Antivirogram® phenotypic assay K70E variants have shown small phenotypic fold change increases for lamivudine and emtricitabine and moderate increases for abacavir, didanosine, stavudine and tenofovir, but below the biological cutoff for these inhibitors (Van Houtte et al., 2006). Interestingly, the K65R and K70E mutations appear to be mutually exclusive and have not been observed to occur together on the same viral

* Corresponding author at: Department of Infectious Diseases, Quest Diagnostics Nichols Institute, 33608 Ortega Hwy, San Juan Capistrano, CA 92675, United States. Tel.: +1 949 728 4018; fax: +1 949 728 4022.
*E-mail address:* Ron.M.Kagan@questdiagnostics.com (R.M. Kagan).

0166-3542/$ – see front matter © 2007 Elsevier B.V. All rights reserved.
doi:10.1016/j.antiviral.2007.03.006

genome (Kagan et al., 2005; Lloyd et al., 2005; Ross et al., 2005; Van Houtte et al., 2006). A recent survey of a large commercial database (Virco BVBA, Mechelen Belgium) of more than 235,000 samples found no instances of K65R and K70E in the same viral sequence in the absence of mixtures (Van Houtte et al., 2006). Similarly, in an earlier study of more than 135,000 samples in the Quest Diagnostics sequence database, we did not detect any occurrence of the K65R and K70E double mutant (Kagan et al., 2005). The K65R + K70E + M184V combination was identified by population sequencing in a single HIV-1 subtype G patient treated with didanosine, lamivudine, abacavir and tenofovir (Delaugerre et al., 2005), however, clonal analysis was not performed on the sample to determine whether these three mutations occurred on the same viral genome.

The ESS30009 study was designed to compare the efficacy of tenofovir or efavirenz co-administered with abacavir and lamivudine as a once-daily fixed-dose combination in treatment-naïve patients (Gallant et al., 2005). The tenofovir/abacavir/lamivudine arm was terminated prior to reaching the 24-week midterm analysis, after an urgent interim analysis was performed due to spontaneous reporting of several cases of early virologic non-response in this arm. An unexpectedly high non-response rate of 49% was observed in this arm, and the K65R mutation had been selected in 54% (22/41) of patients with virologic failures along with M184V/I in 98% (40/41) of these cases (Gallant et al., 2005). A number of subjects on this arm also developed the K70E mutation (Ross et al., 2005). In this work, we present the results of clonal analyses of K70E-containing mutants in the ESS30009 virologic failures and replication capacity results for site-directed mutants (SDM) carrying the K70E and K70E/K65R double mutations. We also carried out molecular dynamic (MD) simulations to better understand the mutual antagonism between the K65R and K70E mutations.

## 2. Methods

### 2.1. ESS30009 study

ESS30009 was a study of 340 ARV-naïve patients randomized to receive a once-daily fixed-dose of abacavir/lamivudine/efavirenz or abacavir/lamivudine/tenofovir. The abacavir/lamivudine/tenfovir arm of this study was discontinued after an unplanned interim analysis of 194 subjects in this arm was performed following spontaneous reports of inadequate response or rebound on this regimen. This unplanned analysis, which occurred prior to all subjects having received 24 weeks of therapy, indicated an unacceptably high incidence of non-response in this arm (Gallant et al., 2005).

### 2.2. Phenotypic analysis, replication capacity and sequencing for ESS30009

Population sequencing and genotyping, plasma HIV-1 drug susceptibility and replication capacity measurements on the baseline and on-therapy samples of the abacavir/lamivudine/tenofovir arm of the ESS30009 study samples were conducted by Monogram Biosciences, South San Francisco, CA (PhenoSense GT™ assay). HIV site-directed mutants containing K70E were created at Monogram Biosciences and analyzed in triplicate for phenotypic impact on study drugs and for replicative capacity.

### 2.3. Clonal analysis of ESS30009 K70E samples

The Monogram Biosciences population sequence data were used to identify samples in which K70E mixtures were detected with K65R mixtures. Plasma containing such mixtures was available from six subjects and these samples were sent to Research Think Tank, Inc. (RTT) for clonal analysis. Clonal analysis was accomplished using HIV-1 GeneTanker™ *PR/RT Select* amplification and nucleotide sequencing methodologies. A minimum of 50 HIV-1 clones were obtained from each of these six samples and analyzed. Briefly, the GeneTanker methodology incorporates unique primers and two-step RT-PCR with cDNA production originating in the 3′ long terminal repeat (LTR), followed by target-specific co-linear amplification. Amplicons for protease and reverse transcriptase were identified, collected, and purified on ethidium-stained 1% agarose gels. Bacterial plasmid clones were obtained by 3′ addition of an A-tail for TA cloning, ligation and transformation using pGEM®-T Vector Systems (Promega Corp. Madison, WI). Approximately 75 isolated colonies selected on IPTG/X-Gal LB agar plates containing 100 μg/ml ampicillin were picked and scaled up by overnight growth in 3 mL Amp100 LB broth. Nucleotide analysis was performed using purified plasmid clones and GeneTanker bi-directional sequencing on the Long-Read Tower™ and OpenGene™ System (Bayer Healthcare, a subsidiary of Bayer AG). Sequence data were exported and electronically transmitted to data management for analysis using the PharmaTanker EMS™ application (Research Think Tank, Inc). Clonal analysis was also performed on one additional sample with K65R and K70E identified by population sequencing, which was submitted to RTT for routine genotypic analysis.

### 2.4. Molecular dynamic simulations

The initial structure used in the MD simulations was based on the crystallographic structure of the HIV-1 reverse transcriptase proposed by Huang et al. (1998) (PDB ID:1RTD). Only the first monomer in the crystal structure was used for the simulation. The positions of hydrogen atoms were determined using the HBUILD facility in the CHARMM simulation program version c32a2 (Brooks et al., 1983). The crystal water molecules were removed and the monomer was capped with a 20 Å sphere of pre-equilibrated TIP3P water molecules (Jorgensen et al., 1983) centered at the ligand. Any water molecule within 2.8 Å of the solute was removed. The ion atmosphere consisted of $Na^+$ and $Cl^-$ ions that were added at random positions to neutralize the system and reach the physiologic sodium concentration of 0.14 M. The ion positions were kept within the water sphere and initially at least 4.7 Å away from any solute atoms.

All mutations were formed by removing the wild-type residue side chain and re-building the mutated residue from the residue

template in CHARMM. Each mutation was treated as an independent simulation: i.e., the simulation for each mutation started from the X-ray structure. Stochastic boundary MD simulations (Brooks et al., 1983, 1985) were carried out. All atoms that were more than 20 Å away from the center of the water sphere were held fixed during the simulations. Atoms within the radial distance of 18 to 20 Å from the center were restrained to the initial X-ray crystal positions.

In MD simulations, the atoms within a sphere of 18 Å from the center were treated with Newtonian dynamics, and the atoms in the radial range between 18 and 20 Å were treated by Langevin dynamics at constant temperature, which also provides a surrounding heatbath for the system. Atomic positions were propagated using the leap-frog Verlet algorithm with 1-fs integration time step (Allen and Tildesley, 1987). Non-bonded interactions were treated using an atom-based cutoff of 14 Å with switching between 10 and 12 Å. Bond lengths for all covalent bonds involving hydrogen were constrained using the SHAKE algorithm (Ryckaert et al., 1977). Initially, a set of simulation annealing processes was applied (total 220 ps simulation). These procedures were to ensure the proper equilibration of water and ion molecules, which is a standard protocol for simulations containing nucleotides or highly charged residues.

#### 2.4.1. Pre-annealing stage

Water and ion molecules were first energy-optimized, then underwent a simulation annealing for 10 ps. The temperature was increased from 0 to 298 K in a 7.5 ps period and was then kept at 298 K. The annealing simulations were repeated twice, with temperature increased from 298 to 498 K and then back to 298 K.

#### 2.4.2. Annealing stage

Four steps of simulations (10 ps each) were performed for this stage:

- The temperature was increased from 298 to 498 K in 7.5 ps and then kept at 498 K.
- The temperature was increased from 498 to 698 K in 7.5 ps and then kept at 698 K.
- The temperature was increased from 698 to 498 K in 7.5 ps and then kept at 498 K.
- The temperature was increased from 498 to 298 K in 7.5 ps and then kept at 298 K.

The whole annealing stage was repeated three times before the post-annealing stage.

#### 2.4.3. Post-annealing stage

Three steps of constant volume simulations were performed in the this stage.

- The temperature was increased from 298 to 498 K in 7.5 ps and then kept at 498 K for a total of 10 ps.
- The temperature was increased from 498 to 298 K in 7.5 ps and then kept at 498 K for a total of 10 ps.
- The temperature was kept at 298 K for 50 ps.

#### 2.4.4. Solute relaxation stage

The solute atoms were energy-optimized and then allowed to move under harmonic restraints during a 50 ps simulation at 298 K. The harmonic force constant (in $\sim$kcal mol$^{-1}$ Å$^{-2}$) on each heavy atom was obtained from the empirical formula $k_i = 25 + 2000/B_i$, where $k_i$ is the force constant for atom i and $B_i$ is the corresponding crystallographic $B$-value.

After the preparation stages, the whole system (within 20 Å from the center) underwent a 500-step energy minimization. Then the temperature was increased from 0 to 298 K at the rate of 1 K/ps and kept at 298 K thereafter. A 10 ns simulation was performed for each mutation and the last 5 ns results were used for data analysis. The data sampling frequency was 1 ps. All average interaction energies and distances were calculated from these 5000 sampled structures for each simulation.

## 3. Results

### 3.1. Clonal analysis of ESS30009 isolates

A virologic non-response rate of 49% was reported for the abacavir/lamivudine/tenofovir arm of the ESS30009 study compared with 5% in the abacavir/lamivudine/efavirenz arm (Gallant et al., 2005). Genotypes at baseline and post-baseline prior to study discontinuation were available for 81 patients in the abacavir/lamivudine/tenofovir arm. No K70E variants were detected at baseline. Population sequencing detected isolates with the K70E substitution in eight of 81 subjects (10%) at post-baseline time points only. In all eight cases, K70E was observed as a mixture of wild-type and mutant (K70K/E) subpopulations. K65K/R mixtures were also observed in the majority of these isolates, and M184V was detected as an apparently homogeneous mutant population in all eight subjects (Table 1). Reduced phenotypic susceptibility to lamivudine was observed in all eight post-baseline isolates. Phenotypic susceptibility for abacavir was reduced in all eight cases but a fold change greater than the abacavir clinical cutoff (4.5) was only observed for three of eight subjects (two of these three subjects had also selected K65R, Y115F, and M184V by population sequencing). Phenotypic susceptibility to tenofovir was retained in all eight non-responders (Table 1). In an attempt to determine genotypic linkage between K65R and K70E, we prepared and analyzed 305 *pol* gene clones from six of these eight patient isolates. Of 305 clones analyzed, K65R and K70E were not observed together on the same clone, whereas M184V was seen in all clones (Table 1).

### 3.2. Site-directed mutant analysis

To further examine whether the K70E and K65R mutations could co-exist in the same virus, we created the following HIV-1 cloned site-directed mutants (SDMs): K70E, K70E + K65R, and K70E + K65R + M184V. Each SDM was analyzed in triplicate for replicative capacity and for phenotypic susceptibility to tenofovir, abacavir and lamivudine (Table 2). Phenotypic resistance of the K70E clone was comparable to previously published results of 1.8-fold for abacavir, 3.7-fold for lamivudine and 1.2-fold for tenofovir in a cell-based assay (Van Houtte et al., 2006)

Table 1
Clonal analysis of six ESS30009 subjects developing K70E

| Subject | Genotype at study initiation[a] | ABC/3TC/TDF at study initiation (FC)[b] | Week | Population genotype at K70E emergence[a] | ABC/3TC/TDF Phenotypic FC[b] at K70E emergence | Clonal analysis[c] | No. of clones |
|---|---|---|---|---|---|---|---|
| 1 | V118I | 1.4/0.6/1.1 | 12 | K70K/E, Y115Y/F, V118I, M184V | 6.5/>124/0.6 | V118I/Y115F/M184V (25)<br>K70E/M184V (4)<br>K65R/M184V (4)<br>T215S/M184V (1)<br>T69N/M184V (3)<br>M184V (14) | 50 |
| 2 | WT | 0.9/0.9/0.9 | 8 | K65K/R, K70K/E, M184V | 3.6/145/0.5 | K70E/M184V (3)<br>K70Q/M184V (1)<br>K65R/M184V (2)<br>M184V (46) | 52 |
| 3 | WT | 0.9/1.2/0.8 | 20 | K65K/R, 70K/E, M184V | 5.1/97/0.9 | K70E/M184V (23)<br>K65R/M184V (31)<br>M184V (2) | 51 |
| 4 | WT | 0.9/0.9/0.8 | 12 | K70K/E, M184V | 4.1/122/0.4 | K70E/M184V (8)<br>K70N/M184V (1)<br>K65R/M184V (2)<br>M184V (39) | 50 |
| 5 | WT | 0.8/1.0/0.9 | 16 | 65K/R, 70K/E, M184V | 3.1/122/0.5 | K70E/M184V (4)<br>K65R/M184V (4)<br>K65R/S68G/M184V (1)<br>V/118I/M184V (1)<br>M184V (40) | 50 |
| 6 | WT | 1.0/0.9/0.7 | 20 | K65K/R, K70K/E, Y115Y/F, M184V | 7.8/85/0.6 | T69S/F77S/Y115F/M184V (1)<br>K70E/Y115F/M184V (1)<br>K65R/Y115F/M184V (1)<br>Y115F/M184V (45)<br>K103R/M184V (1)<br>M184V (2) | 51 |
| 7 | WT | 0.8/0.9/0.9 | 16 | K65K/R, K70K/E, M184V | 2.7/114/0.5 | ND[d] | ND[d] |
| 8 | WT | 1.1/0.9/1.1 | 16 | K65K/R, K70K/E, M184M/I/V | 3.2/114/0.6 | ND[d] | ND[d] |

Eight of 81 subjects in the abacavir/lamivudine/tenofovir (ABC/3TC/TDF) arm of the ESS30009 study developed the K70E mutation as detectable by population sequencing. Clonal analysis was carried out for 305 clones from six of these patients and did not detect K65R and K70E on the same genome.

[a] Population sequencing was performed at Monogram Biosciences (PhenoSense GT™ assay). Samples with no IAS USA-defined RT inhibitor resistance mutations are designated as wild-type.

[b] FC: fold change. Phenotypic susceptibility analysis was performed at Monogram Biosciences (PhenoSense GT™ assay).

[c] Clonal analysis was conducted at Research Think Tank, Inc. using the Gene Tanker™ methodologies.

[d] ND: not done.

Table 2
Mean fold change in drug susceptibility and replicative capacity in HIV-1 with site-directed mutations

| Site-directed mutant | Phenotypic fold change[a] | | | Replication capacity[a] (%) |
|---|---|---|---|---|
| | Abacavir | Lamivudine | Tenofovir | |
| K70E | 1.4 ± 0.05 | 3.4 ± 0.1 | 1.2 ± 0.09 | 97.3 ± 29 |
| K65R + K70E | 3.1 ± 0.4 | 8.8 ± 0.8 | 2.3 ± 0.4 | 2.4 ± 0.9 |
| K65R + K70E + M184V | NA[b] | NA[b] | NA[b] | 0.01 ± 0.01 |

Site-directed mutants were constructed by Monogram Biosciences as described in Methods. Phenotypic fold change and replication capacity analyses were conducted in triplicate using the PhenoSense™ assay. Phenotypic analysis of a K65R site-directed mutant was not performed in this study, however the mean fold change in 147 clinical isolates with only the K65R NRTI mutation is reported to be 1.9 for tenofovir, 2.5 for abacavir and 8.5 for 3TC, and the mean replication capacity of these isolates was 68% (Underwood et al., 2004).

[a] Mean and standard deviation for three measurements.

[b] The replication capacity was too low to measure $IC_{50}$ values for phenotypic determination of fold change.

or derived from pre-steady state kinetic measurements (2.3×, 3.5× and 2.1×, respectively; Sluis-Cremer et al., 2007). No additive affect on phenotypic resistance was observed for the double mutant (Table 2). Phenotypic resistance values were comparable to values reported for K65R alone for abacavir which is typically around three-fold, lamivudine, reported at 7.7-fold, and tenofovir, reported at 2.7-fold (Deval et al., 2004). Unlike K65R mutants, which are reported to have reduced replication capacity of 58% (Deval et al., 2004) to 69% (White et al., 2002), the replication capacity of the K70E SDM did not differ from that of the wild-type control (Table 2). However, in the double mutant K65R + K70E, the replication capacity declined to <2.4% (Table 2). M184V has been reported to reduce the replication capacity of the K65R mutant to 38% of wild-type (Deval et al., 2004). In the triple mutant K65R + K70E + M184V, replication capacity was reduced to a nearly undetectable <0.01% of wild-type (Table 2).

### 3.3. Molecular dynamic simulations

To better understand the large reductions in replication capacity observed in the K65R + K70E double mutants, we conducted MD simulations of wild-type and mutant RT bound to dTTP, starting with the coordinates for the 1RTD structure from Huang et al. (1998). The main chain root mean square deviations between the MD simulations and the 1RTD structure were small, between 0.92 and 1.4 Å (Table 3). Key distances and interaction energies between the ligand and key residues were calculated from the MD simulation trajectories (Tables 3 and 4). Snapshots of the models at 6 ns were taken to demonstrate the relative positions of the ligand and key residues (Fig. 1).

In the wild-type RT crystallized with dTTP, the ε-amino group of K65 interacts with the γ-phosphate of dTTP. The loss of this interaction in the R65 mutant likely introduces unfavorable rearrangements (Huang et al., 1998). In the wild-type MD simulation of RT with the dTTP ligand, the ζ-nitrogen of K65 (K65:Nζ) can interact with the γ-phosphate oxygen of dTTP (dTTP:Oγ) from a distance of 2.7 ± 0.1 Å, whereas the K70 side chain ζ-nitrogen (K70:Nζ) is distant (6.6 ± 1.1 Å) from the γ-phosphate oxygen (Fig. 1a, Table 4). This residue 65-γ-phosphate interaction was not observed in the R65 single-mutant MD simulation, where the guanidinium nitrogen of R65 (R65:Nη) was 4.2 ± 0.4 Å distant from dTTP:Oγ (Fig. 1b, Table 4) and there was a +55 kcal/mol unfavorable change in interaction energy (Table 3). However, in this model, K70:Nζ was repositioned much closer to the ligand, 3.5 ± 0.6 Å distant from dTTP:Oγ, and may partially compensate for the loss of the K65 interaction with the ligand (Fig. 1b) as evidenced by the −67 kcal/mol more favorable interaction energy between K70 and the ligand (Table 3). In the simulation of the E70 mutant (Fig. 1c) the carboxyl oxygen of E70 (E70:Oγ) moved closer to within 2.7 ± 0.1 Å of the positively charged ε-amino group of K65, creating an electrostatic interaction. However, the interaction of K65:Nζ with the γ-phosphate of the ligand did not appear to be lost and it was positioned 2.7 ± 0.1 Å from dTTP:Oγ and the interaction energy between K65 and the ligand was comparable to that in the wild-type model (Tables 3 and 4). R65:Nη was closer to dTTP:Oγ in the R65 + E70 double mutant (3.0 ± 0.2 Å) when compared to the R65 single mutant (4.2 ± 0.4 Å) (Fig. 1d, Table 4), but the interaction energy between R65 and the ligand was +30 kcal/mol less favorable than in the wild-type model and there was no compensating interaction of the ligand with the negatively charged E70 (Table 3).

In the crystal structure, the triphosphate moiety of the ligand is also coordinated by the side chain of R72 and the main chain nitrogen of D113 (Huang et al., 1998; Harris et al., 1998). The guanidinium group of R72 was farther away from the α-phosphate in the E70 single mutant (Fig. 1c and d, Table 4) and was within hydrogen-bonding distance in only 1.34% of the

Table 3
R.M.S. deviations and key interaction energies between residues 65/70 and the ligand

| | R.M.S.D. (Å) | Residue 65 (kcal/mol) | Residue 70 (kcal/mol) |
|---|---|---|---|
| WT | 0.92 ± 0.1 | −166 ± 7 | −62 ± 17 |
| K65R | 1.45 ± 0.1 | −111 ± 9 | −129 ± 19 |
| K70E | 1.07 ± 0.1 | −169 ± 6 | 91 ± 7 |
| K65R/K70E | 0.92 ± 0.1 | −136 ± 8 | 90 ± 11 |

Root Mean Square deviation (R.M.S.) was calculated for atoms within a 18 Å sphere around the ligand for each model and the starting crystal structure of HIV-1 with a dTTP ligand (PDB ID: 1RTD) from Huang et al. (1998). The interaction energies between two residues are defined as the summation of electrostatic energies and van der Waals interactions between every atom pair from different residues. They were calculated by the INTERACTION module in the CHARMM program. Interaction energies were averaged over the last 5000 sampled structures sampled at 1 ps intervals.

Table 4
Key dNTP binding pocket residue to dTTP ligand distances

| | K65:Nζ ↔ dTTP:Oγ[a] | R65:Nη ↔ dTTP:Oγ | K70:Nζ ↔ dTTP:Oγ | E70:Oγ ↔ dTTP:Oγ | R65:Nη ↔ E70:Oγ | K65:Nζ ↔ E70:Oγ | R72:NηH ↔ dTTP:Oα[b] |
|---|---|---|---|---|---|---|---|
| WT | 2.7 ± 0.1 | | 6.6 ± 1.1 | | | | 3.0 ± 1.0 |
| K65R | | 4.2 ± 0.4 | 3.5 ± 0.6 | | | | 3.4 ± 0.5 |
| K70E | 2.7 ± 0.1 | | | 4.4 ± 0.5 | | 2.7 ± 0.1 | 5.3 ± 0.9 |
| K65R/K70E | | 3.0 ± 0.2 | | 4.6 ± 0.7 | 3.6 ± 0.6 | | 2.5 ± 0.5 |

All distances were calculated from the last 5 ns of simulations of the WT, K65R, K70E and K65R/K70E models with the dTTP ligand. A 1 ps sampling rate was used, giving 5000 measurements for each distance. The distances (Å) and standard deviations are shown.

[a] The minimum possible distance was used when multiple choices existed, as in the case of the two Oγ in the E70 side chain.

[b] R72:NηH was within hydrogen-bonding distance (<3.5 Å) of the α-phosphate in only 1.34% of the simulations for the E70 mutant but in 95.4% of the double mutant and, 56% of the wild-type and 51% of the R65 simulations.

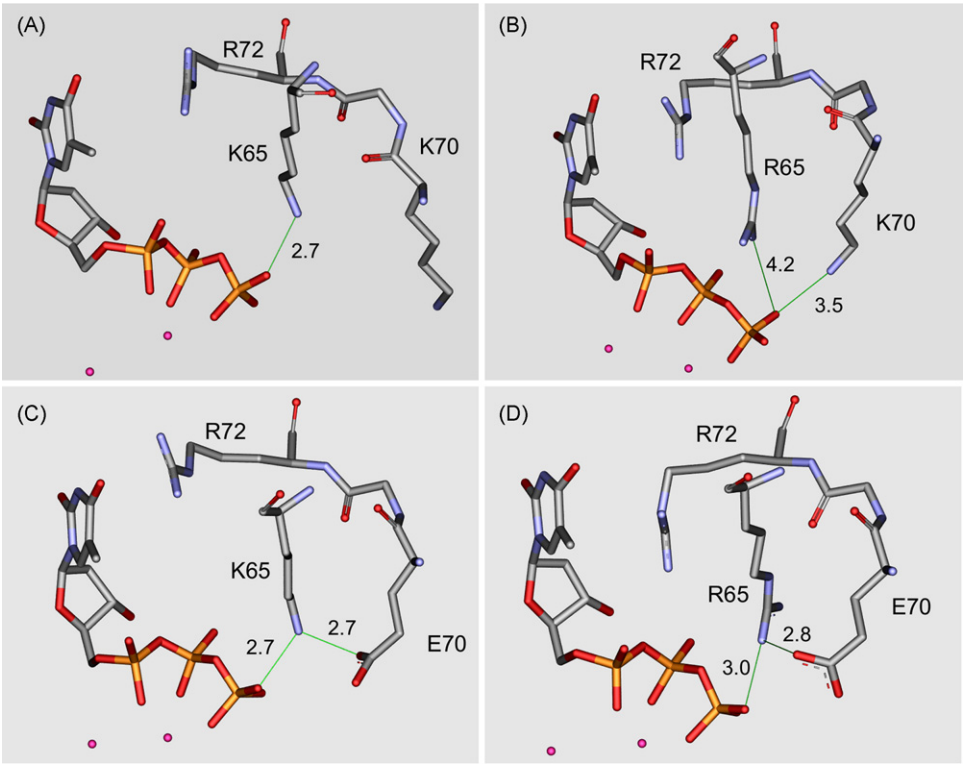


Fig. 1. Molecular dynamic snapshot at 6 ns of the dTTP ligand and residues 65, 70, 71 (backbone only) and 72 in single and double mutant RT. DS Visualizer™ version 1.6 (Accelrys Software, Inc. San Diego, CA) was used to prepare the figure. (A) Wild-type model. (B) K65R mutant. (C) K70E mutant. (D) K65R + K70E double mutant. Interatomic distances are given in Angstrom units (Å) and are average distances as shown in Table 4.

simulations. In the double mutant, R72 remained close to the α-phosphate (Fig. 1c and d, Table 4) and was more likely to be within hydrogen-bonding distance (double mutant: 95.4%; wild-type: 56.0%; K65R: 51.0%). We did not observe any repositioning in the main chain nitrogen of D113 relative to the triphosphate moiety in any of the wild-type or mutant MD simulations (data not shown).

## 4. Discussion

Following the widely publicized findings that certain triple-NRTI combination therapies that included tenofovir and abacavir lead to an increased rate of virologic failure and selection of the K65R mutation (Gallant et al., 2005; Khanlou et al., 2005; Landman et al., 2005; Leon et al., 2005; Maitland et al., 2005; Torti et al., 2005), the prevalence of K65R has declined from its peak of 4.5% in 2003. The emergence of the adefovir-associated resistance mutation K70E in patients failing treatment with tenofovir and other NRTIs was first reported in 2005 (Delaugerre et al., 2005; Rouse et al., 2005; Lloyd et al., 2005). Recently published work (Sluis-Cremer et al., 2007) shows that K70E confers low-level resistance to tenofovir by selectively reducing the incorporation efficiency of nucleoside RT inhibitors, similar to the K65R mechanism of action (Deval et al., 2004). Both mutations also impair the excision pathway of thymidine analog mutation mediated resistance for thymidine analogs such as azidothymidine (White et al., 2006; Sluis-Cremer et al., 2007).

In this work, we confirmed that the absence of K65R + K70E double mutants in large clinical populations was not simply an artifact of failure to detect such mutants in population-based sequencing assays. Clonal analysis of virologic non-responders in the abacavir/lamivudine/tenofovir arm of the ESS30009 study who had detectable K70E and K65R mixtures failed to identify any double mutants. Recombinant viruses carrying the double mutant had phenotypic resistance levels comparable to K65R alone with no additive affect, but the double mutant had a much greater loss of replicative capacity than either of the single mutants, suggesting that this combination would be unfavorable. Since in the clinical samples analyzed by clonal sequencing, K70E was always accompanied by M184V on the same clone, and given that the site-directed triple recombinants carrying the M184V mutation had a replication capacity nearly too low to measure (0.01%), these findings suggest that while K70E might be observed by population sequencing with K65R in clinical isolates, it would be less likely for both mutations to be selected on the same viral genome in a clinical sample. K70E is still very rare and much less prevalent than K65R in the clinical population, which suggests that in vivo, the K65R mutation is the preferred pathway to loss of susceptibility to tenofovir.

To better understand the deleterious effects of the double mutation on the viral reverse transcriptase, we undertook MD simulations of K65R, K70E and K65R + K70E reverse transcriptase with bound dTTP ligand. Positioning and coordination of the nucleotide triphosphate ligand in the nucleotide binding pocket of the reverse transcriptase is important for phosphodi-

ester bond formation, which proceeds through the attack of the 3′-OH of the primer on the α-phosphate of the dNTP followed by the leaving of the terminal pyrophosphate group (Jacobo-Molina et al., 1993). Mutations that affect ligand binding by reducing the rate of incorporation of dNTPs and nucleoside/nucleotide analog inhibitors include M184V (Krebs et al., 1997; Deval et al., 2004), K65R (Selmi et al., 2001; Deval et al., 2004) and Q151M (Deval et al., 2002). The γ-phosphate of the nucleotide ligand is stabilized by the amino group side chain of K65, and the K65R substitution may abolish this stabilization and induce packing rearrangements in the vicinity of the β- and γ-phosphates (Huang et al., 1998; Sarafianos et al., 1999). We used MD simulations to demonstrate that the guanidinium nitrogen of R65 is farther from the γ-phosphate compared to the amino group of K65 in the wild-type variant and that the interaction energy between these moieties becomes less favorable, in agreement with the predicted loss of interaction. Interestingly, the amino group side chain of K70, which is distant from the ligand in the wild-type model, is shifted much closer to the γ-phosphate with a more favorable interaction energy with the ligand. This previously undescribed interaction may partially compensate for the loss of γ-phosphate stabilization when the lysine at position 65 is substituted by arginine. Nevertheless, the replication capacity of R65 variants is reduced, indicating that these changes still have a deleterious affect on the reverse transcriptase.

In the double mutant, the negatively charged glutamate at position 70 cannot interact with the γ-phosphate of the ligand to compensate for the loss of the interaction with residue 65, and we postulate that this results in a more severe defect than that caused by the single R65 mutation. Although R65 appears closer to the γ-phosphate in the double mutant, its interaction energy with the ligand is 30 kcal/mol less favorable than K65 in either the wild-type or the E70 single mutant; therefore, it does not appear to provide much stabilization of the γ-phosphate. We speculate that the γ-phosphate may preferentially interact with the adjacent negatively charged E70, which may prevent it from stabilizing the γ-phosphate. In the single mutant K70E, the E70 carboxylate is close enough to the positively charged amino group of K65 to form a salt bridge, and as recently suggested (Sluis-Cremer et al., 2007) this may affect the interaction of K65 with the γ-phosphate. Alternately, the repositioning of R72:NηH outside of the normal hydrogen-bonding distance with the ligand α-phosphate may in itself destabilize the pyrophosphate leaving group sufficiently to account for the poorer incorporation of nucleosides and nucleoside analogs and the resultant low-level resistance observed in K70E variants. R72A mutants exhibit very poor catalytic activity (Harris et al., 1998) suggesting that structural changes impacting this residue could also have an effect on activity.

Although both K65R and M184V reduce the rate of nucleotide incorporation, K65R does so by reducing the catalytic rate constant whereas M184V reduces the binding affinity of the nucleotide. When present together, these mutations can act synergistically to reduce the rate of incorporation of the nucleotide (Deval et al., 2004). This synergistic interaction may account for the greater loss of replicative capacity that we observed in the triple mutant. MD simulations of the triple mutant with purine and pyrimidine dNTP ligands may shed further light on the additional fitness loss.

Although our study represents the longest all-atom simulation reported to-date for an HIV-1 RT system, the results must be treated with caution. Our simulations were based on cutoff models; i.e., we only simulated the region near the active site, and did not employ the most advanced techniques for treating non-bonding interactions such as long-range electrostatic interactions. Hence quantitative analyses were not possible and long range conformational changes would not be captured. Thus, our simulation results are intended to be used for interpreting the experimental evidence, rather than for de novo prediction of mutational effects. These analytical limitations are due to the limitations in currently available computational power. A full-scale and predictive MD study of the HIV-1 RT system may be become possible with further advances in computer hardware and software.

## 5. Conclusions

In summary, we have proposed a mechanistic explanation for the incompatibility of two reverse transcriptase mutations, K65R and K70E, consistent with the reduced replication capacity of site-directed double mutants and the reported absence of such double mutants in clinical databases in spite of the widespread use of tenofovir. MD simulations have been used previously in structural studies of the HIV-1 RT dNTP binding site and nucleotide analog resistance (White et al., 2004, 2006). MD simulations, by their nature, are computationally expensive and therefore are usually limited to defined shells encompassing regions of interest in biological macromolecules and limited in duration to hundreds of picoseconds or several nanoseconds. In this work, we were able to model an 18–20 Å shell around the dNTP binding site of RT and conduct relatively long-duration (10 ns) simulations. This technique allowed us to study changes in atomic-level motions in the nucleotide-binding site of HIV-1 reverse transcriptase resulting from the introduction of specific drug resistance mutations. Further applications of this methodology may serve to provide a better mechanistic understanding of additional single or combined mutations in the nucleotide binding site of the HIV-1 reverse transcriptase including further antagonistic interactions such as between K65R or K70E and thymidine analog mutations (White et al., 2006; Sluis-Cremer et al., 2007) or between K65R and L74V (Sharma et al., 2004).

## Acknowledgements

The authors would like to thank N. Parkin, K. Limoli and W. Huang of Monogram BioSciences for the site-directed mutant creation and analysis, P. Gerondelis, E. Rouse, M. Lim and R. Lanier of Glaxo Smithkline for their help with the ESS30009 study and clonal analysis and J.T. Huong, D.A. Burns and B.D. Kirkpatrick of Research Think Tank Inc. for their contributions to the clonal analysis in this work. The authors also wish to thank Jeff Radcliff (Quest Diagnostics Nichols Institute, San Juan Capistrano, CA) for carefully reviewing and editing the manuscript. This work was partially supported by

the National Center for Supercomputing Applications (NCSA) under MCB050050N and utilized NCSA's IBM p690 (copper) machine.

## References


Allen, M.P., Tildesley, D.J., 1987. Computer Simulation of Liquids. Oxford Science Publications, Oxford.

Brooks, B.R., Bruccoleri, R.E., Olafson, B.D., States, D.J., Swaminathan, S., Karplus, M., 1983. CHARMM: a program for macromolecular energy, minimisation and dynamics calculations. Comput. Chem. 4, 187–217.

Brooks 3rd, C.L., Brunger, A., Karplus, M., 1985. Active site dynamics in protein molecules: a stochastic boundary molecular-dynamics approach. Biopolymers 24, 843–865.

Camacho, R., Theys, K., Abecasis, A., Deforche, K., Carvalho, A.P., Cabanas, J., Gomes, P., Vandamme, A.-M., 2006. Rise and fall of the RT K65R incidence in the Portuguese resistance database. Antiviral Ther. 11, S134.

Cherrington, J.M., Mulato, A.S., Fuller, M.D., Chen, M.S., 1996. Novel mutation (K70E) in human immunodeficiency virus type 1 reverse transcriptase confers decreased susceptibility to 9-[2-(phosphonomethoxy)ethyl]adenine in vitro. Antimicrob. Agents Chemother. 40, 2212–2216.

Delaugerre, C., Roudiere, L., Peytavin, G., Rouzioux, C., Viard, J.P., Chaix, M.L., 2005. Selection of a rare resistance profile in an HIV-1-infected patient exhibiting a failure to an antiretroviral regimen including tenofovir DF. J. Clin. Virol. 32, 241–244.

Deval, J., Selmi, B., Boretto, J., Egloff, M.P., Guerreiro, C., Sarfati, S., Canard, B., 2002. The molecular mechanism of multidrug resistance by the Q151M human immunodeficiency virus type 1 reverse transcriptase and its suppression using alpha-boranophosphate nucleotide analogues. J. Biol. Chem. 277, 42097–42104.

Deval, J., White, K.L., Miller, M.D., Parkin, N.T., Courcambeck, J., Halfon, P., Selmi, B., Boretto, J., Canard, B., 2004. Mechanistic basis for reduced viral and enzymatic fitness of HIV-1 reverse transcriptase containing both K65R and M184V mutations. J. Biol. Chem. 279, 509–516.

Faruki, H., Sebastian, J., Scott, J., Stamp, J., Lanier, E.R., 2004. Changes in prevalence of NRTI resistance associated mutations among clinical isolates from 1999–2003. Antiviral Ther. 9, S91.

Gallant, J.E., Rodriguez, A.E., Weinberg, W.G., Young, B., Berger, D.S., Lim, M.L., Liao, Q., Ross, L., Johnson, J., Shaefer, M.S., 2005. Early virologic nonresponse to tenofovir, abacavir, and lamivudine in HIV-infected antiretroviral-naive subjects. J. Infect. Dis. 192, 1921–1930.

Harris, D., Kaushik, N., Pandey, P.K., Yadav, P.N., Pandey, V.N., 1998. Functional analysis of amino acid residues constituting the dNTP binding pocket of HIV-1 reverse transcriptase. J. Biol. Chem. 273, 33624–33634.

Huang, H., Chopra, R., Verdine, G.L., Harrison, S.C., 1998. Structure of a covalently trapped catalytic complex of HIV-1 reverse transcriptase: implications for drug resistance. Science 282, 1669–1675.

Jacobo-Molina, A., Ding, J., Nanni, R.G., Clark Jr., A.D., Lu, X., Tantillo, C., Williams, R.L., Kamer, G., Ferris, A.L., Clark, P., et al., 1993. Crystal structure of human immunodeficiency virus type 1 reverse transcriptase complexed with double-stranded DNA at 3.0 A resolution shows bent DNA. Proc. Natl. Acad. Sci. U.S.A. 90, 6320–6324.

Jorgensen, W.L., Chandrasekhar, J., Madura, J.D., 1983. Comparison of simple potential functions for simulating liquid water. J. Chem. Phys. 79, 926–935.

Kagan, R., Ross, L., Winters, M., Merigan, T., Heseltine, P., Lewinski, M., 2005. Adefovir-associated HIV-1 RT mutation K70E in the age of tenofovir. Antiviral Ther. 10, S103.

Kagan, R.M., Merigan, T.C., Winters, M.A., Heseltine, P.N., 2004. Increasing prevalence of HIV-1 reverse transcriptase mutation K65R correlates with tenofovir utilization. Antiviral Ther. 9, 827–828.

Khanlou, H., Yeh, V., Guyer, B., Farthing, C., 2005. Early virologic failure in a pilot study evaluating the efficacy of therapy containing once-daily abacavir, lamivudine, and tenofovir DF in treatment-naive HIV-infected patients. AIDS Patient Care STDS 19, 135–140.

Krebs, R., Immendorfer, U., Thrall, S.H., Wohrl, B.M., Goody, R.S., 1997. Single-step kinetics of HIV-1 reverse transcriptase mutants responsible for virus resistance to nucleoside inhibitors zidovudine and 3-TC. Biochemistry 36, 10292–10300.

Landman, R., Descamps, D., Peytavin, G., Trylesinski, A., Katlama, C., Girard, P.M., Bonnet, B., Yeni, P., Bentata, M., Michelet, C., Benalycherif, A., Brun Vezinet, F., Miller, M.D., Flandre, P., 2005. Early virologic failure and rescue therapy of tenofovir, abacavir, and lamivudine for initial treatment of HIV-1 infection: TONUS study. HIV Clin. Trials 6, 291–301.

Leon, A., Mallolas, J., Martinez, E., De Lazzari, E., Pumarola, T., Larrousse, M., Milincovic, A., Lonca, M., Blanco, J.L., Laguno, M., Biglia, A., Gatell, J.M., 2005. High rate of virological failure in maintenance antiretroviral therapy with didanosine and tenofovir. AIDS 19, 1695–1697.

Lloyd, R., Huong, J., Rouse, E., Gerondelis, P., Lim, M., Shaefer, M., Rodriguez, A., Gallant, J., Lanier, R., Ross, L., 2005. HIV-1 RT mutations K70E and K65R are not present on the same viral genome when both mutations are detected in plasma. In: 45th Interscience Conference on Antimicrobial Agents and Chemotherapy, Washington, DC, USA, December 16–19.

Maitland, D., Moyle, G., Hand, J., Mandalia, S., Boffito, M., Nelson, M., Gazzard, B., 2005. Early virologic failure in HIV-1 infected subjects on didanosine/tenofovir/efavirenz: 12-week results from a randomized trial. AIDS 19, 1183–1188.

Miller, M.D., Margot, N.A., Lamy, P.D., Fuller, M.D., Anton, K.E., Mulato, A.S., Cherrington, J.M., 2001. Adefovir and tenofovir susceptibilities of HIV-1 after 24 to 48 weeks of adefovir dipivoxil therapy: genotypic and phenotypic analyses of study GS-96-408. J. Acquir. Immune Defic. Syndr. 27, 450–458.

Parikh, U.M., Bacheler, L., Koontz, D., Mellors, J.W., 2006. The K65R mutation in human immunodeficiency virus type 1 reverse transcriptase exhibits bidirectional phenotypic antagonism with thymidine analog mutations. J. Virol. 80, 4971–4977.

Parikh, U.M., Koontz, D.L., Chu, C.K., Schinazi, R.F., Mellors, J.W., 2005. In vitro activity of structurally diverse nucleoside analogs against human immunodeficiency virus type 1 with the K65R mutation in reverse transcriptase. Antimicrob. Agents Chemother. 49, 1139–1144.

Ross, L., Gerondelis, P., Liao, Q., Wine, B., Lim, M., Shaefer, M., Rodriguez, A., Limoli, K., Huang, W., Parkin, N.T., Gallant, J., Lanier, R., 2005. Selection of the HIV-1 reverse transcriptase mutation K70E in antiretroviral-naive subjects treated with tenfovir/abacavir/lamivudine therapy. Antiviral Ther. 10, S102.

Rouse, E., Gerondelis, P., Paulsen, D., Underwood, M., McClermon, D., Preble, L., McCarville, J., Lim, M., Shaefer, M., Rodriguez, A., Gallant, J., Liao, Q., Lanier, R., Ross, L., 2005. Clonal analysis of week 12 virologic non-responders receiving tenofovir/abacavir/lamivudine in ESS30009. In: 12th Conference on Retroviruses and Opportunistic Infections, Boston, MA, USA, February 22–25.

Ryckaert, J.P., Ciccotti, G., Berendsen, H.J.C., 1977. Numerical integration of the Cartesian equations of motion of a system with constraints: molecular dynamics of n-alkanes. J. Comp. Phys. 23, 327–341.

Sarafianos, S.G., Das, K., Ding, J., Boyer, P.L., Hughes, S.H., Arnold, E., 1999. Touching the heart of HIV-1 drug resistance: the fingers close down on the dNTP at the polymerase active site. Chem. Biol. 6, R137–R146.

Selmi, B., Boretto, J., Sarfati, S.R., Guerreiro, C., Canard, B., 2001. Mechanism-based suppression of dideoxynucleotide resistance by K65R human immunodeficiency virus reverse transcriptase using an alpha-boranophosphate nucleoside analogue. J. Biol. Chem. 276, 48466–48472.

Sharma, P.L., Nurpeisov, V., Lee, K., Skaggs, S., Di San Filippo, C.A., Schinazi, R.F., 2004. Replication-dependent 65R–>K reversion in human immunodeficiency virus type 1 reverse transcriptase double mutant K65R + L74V. Virology 321, 222–234.

Sluis-Cremer, N., Sheen, C.W., Zelina, S., Torres, P.S., Parikh, U.M., Mellors, J.W., 2007. Molecular mechanism by which the K70E mutation in human immunodeficiency virus type 1 reverse transcriptase confers resistance to nucleoside reverse transcriptase inhibitors. Antimicrob. Agents Chemother. 51, 48–53.

Torti, C., Quiros-Roldon, E., Regazzi, M., Antinori, A., Patroni, A., Villani, P., Tirelli, V., Cologni, G., Zinzi, D., Lo Caputo, S., Perini, P., Carosi, G., 2005. Early virological failure after tenofovir + didanosine + efavirenz combination in HIV-positive patients upon starting antiretroviral therapy. Antiviral Ther. 10, 505–513.

Underwood, M.R., Ross, L., Irlbeck, D., Gerondelis, P., St Clair, M.H., Lan Trinh, L., Parkin, N., Lanier, E.R., 2004. Sensitivity of Phenotypic Analyses for detection of low levels of K65R, M184V, or K65R/M184V in mixtures with wild-type HIV-1. Antiviral Therapy 9, S144.

Van Houtte, M., Staes, M., Geretti, A.M., Pattery, T., Bacheler, L., 2006. NRTI resistance associated with the RT mutation K70E in HIV-1. Antiviral Ther. 11, S160.

Wainberg, M.A., Miller, M.D., Quan, Y., Salomon, H., Mulato, A.S., Lamy, P.D., Margot, N.A., Anton, K.E., Cherrington, J.M., 1999. In vitro selection and characterization of HIV-1 with reduced susceptibility to PMPA. Antiviral Ther. 4, 87–94.

White, K.L., Chen, J.M., Feng, J.Y., Margot, N.A., Ly, J.K., Ray, A.S., Macarthur, H.L., McDermott, M.J., Swaminathan, S., Miller, M.D., 2006. The K65R reverse transcriptase mutation in HIV-1 reverses the excision phenotype of zidovudine resistance mutations. Antiviral Ther. 11, 155–163.

White, K.L., Chen, J.M., Margot, N.A., Wrin, T., Petropoulos, C.J., Naeger, L.K., Swaminathan, S., Miller, M.D., 2004. Molecular mechanisms of tenofovir resistance conferred by human immunodeficiency virus type 1 reverse transcriptase containing a diserine insertion after residue 69 and multiple thymidine analog-associated mutations. Antimicrob. Agents Chemother. 48, 992–1003.

White, K.L., Margot, N.A., Wrin, T., Petropoulos, C.J., Miller, M.D., Naeger, L.K., 2002. Molecular mechanisms of resistance to human immunodeficiency virus type 1 with reverse transcriptase mutations K65R and K65R + M184V and their effects on enzyme function and viral replication capacity. Antimicrob. Agents Chemother. 46, 3437–3446.